Advances and New Directions in Crystallization Control

Zoltan K. Nagy[1] and Richard D. Braatz[2]

[1]Department of Chemical Engineering, Loughborough University, Loughborough, LE11 3TU, United Kingdom; email: z.k.nagy@lboro.ac.uk

[2]Department of Chemical Engineering, Massachusetts Institute of Technology, Cambridge, Massachusetts 02139; email: braatz@mit.edu

Annu. Rev. Chem. Biomol. Eng. 2012. 3:55–75

First published online as a Review in Advance on March 8, 2012

The *Annual Review of Chemical and Biomolecular Engineering* is online at chembioeng.annualreviews.org

This article's doi: 10.1146/annurev-chembioeng-062011-081043

1947-5438/12/0715-0055$20.00

Keywords

pharmaceuticals, particulate processing, process control, polymorphism, microfluidics, model predictive control

Abstract

The academic literature on and industrial practice of control of solution crystallization processes have seen major advances in the past 15 years that have been enabled by progress in in-situ real-time sensor technologies and driven primarily by needs in the pharmaceutical industry for improved and more consistent quality of drug crystals. These advances include the accurate measurement of solution concentrations and crystal characteristics as well as the first-principles modeling and robust model-based and model-free feedback control of crystal size and polymorphic identity. Research opportunities are described in model-free controller design, new crystallizer designs with enhanced control of crystal size distribution, strategies for the robust control of crystal shape, and interconnected crystallization systems for multicomponent crystallization.

INTRODUCTION AND BACKGROUND

ATR-FTIR: attenuated total reflection-Fourier transform infrared

Crystallization from solution is ubiquitous in many industries including fine chemicals, food, and pharmaceuticals. Typically, evaporation, cooling, or the addition of solvents, precipitants, or other chemicals are used to create the supersaturated solution that induces enough solute molecules to come together to nucleate and grow crystals. The control of solution crystallization processes has been studied since the 1940s but did not really take off until the 1990s (1, 2). Several factors have motivated the growth in research publications and industrial applications since the 1990s: (*a*) in situ real-time sensor technologies such as attenuated total reflection-Fourier transform infrared (ATR-FTIR) spectrometry and laser backscattering probes that could provide much richer data sets suitable for crystallization modeling and control became commercially available; (*b*) computers and control hardware became faster, which enabled the application of population balance modeling and the investigation and implementation of advanced techniques for systems and control; and (*c*) manufacturing drug crystals of higher consistency and quality became more important, and several pharmaceutical companies and governments were willing to invest in research programs to develop improved methods for crystallizer control (3).

During the 1990s and early 2000s, it was recognized that prior model-based optimal control formulations for solution crystallization processes in the literature had serious problems that limited their applicability, namely:

1. Usually the optimization variable for seeded batch crystallizations in the earlier studies was the temperature profile, whereas the characteristics of the seed crystals were ignored even though they have at least as strong of an effect on the product crystal properties as the temperature profile (4–6).
2. The most commonly used optimization objectives were the minimization of the coefficient of variation and the maximization of the weight-mean size of the product crystals. These objectives could produce large numbers of small crystals that could cause downstream filtration problems and could lead to operations that are highly sensitive to model uncertainties (4–12).
3. Uncertainties in crystallization kinetics and the effects of disturbances were nearly always ignored, although all of the benefits to product quality owing to optimization could be lost if uncertainties and disturbances were not taken into account (10).
4. Optimal controls designed to minimize nucleation did not explicitly consider a key operational constraint, namely that the supersaturation should be less than the metastable limit, which is the supersaturation in which excessive nucleation occurs. Because the metastable limit information was included only indirectly through the specification of the nucleation kinetics (13), the above formulation limitations took much longer to notice. Later papers often plot the optimal control trajectory in the crystallization phase diagram so that the distance between the operations and the metastable limit is easily visualized (14–16).

By the late 1990s, control designs were being developed that did not have the above limitations, and crystallization control systems became relevant to and implemented in industrial practice through tight partnerships formed between industrial and academic research laboratories. This review focuses primarily on the subsequent advances in crystallization control that occurred in the past decade or so as well as opportunities for further promising future research directions.

ADVANCES

Accurate In Situ Real-Time Measurement of Solution Concentrations in Multicomponent Crystallizations

Probably the most important enabler of modern crystallization process control was ATR-FTIR spectroscopy. Traditional FTIR spectroscopy, which directs light through the entire medium

being measured, is not directly applicable to crystal slurries because the crystals block the light beam such that no signal reaches the detector. In ATR spectroscopy, solid, liquid, or gas phases can be measured directly using an ATR crystal. A light beam passes through the ATR crystal such that on its way back to the detector, the beam reflects at least once off of the internal surface of the crystal in contact with the medium being measured. An evanescent wave is created that extends into the medium approximately 1–10 micrometers, and the light beam is affected by the medium within this evanescent wave. In the 1990s ATR probes of approximately 1 inch in diameter were available that could be easily inserted into a vessel or pipe of liquid solution to track in situ and in real-time changes in the infrared absorption spectrum, which could be correlated with solution concentrations. These ATR probes had bases that plugged into standard FTIR spectrometers for a relatively low cost. A key innovation was the recognition that an ATR-FTIR probe could be employed to track the liquid solution concentrations in industrial crystallizers (17, 18) because the penetration depth of the evanescent wave was sufficiently small that the proportion of medium within the wave that is crystals in a forced convection would be small owing to steric, hydrodynamic, and other forces (19).

Although the feasibility of this approach was first demonstrated in the mid-1990s (17), transfer of the technology into industrial practice took several years because the measurement accuracies obtained in industrial and academic research laboratories were too low for effective application in crystallization process modeling and control. Four changes to the original protocol improved the experimental design and data analysis by more than an order of magnitude, namely (20):

1. The use of absorbances for many wavenumbers instead of a single transmittance ratio in the sensor calibration. Absorbances have the advantage of being approximately linearly related to the solution concentrations, which simplifies the construction of a calibration model, and the use of many wavenumbers allows for averaging of the effects on the solution concentration measurement of noise and the small proportion of crystals within the evanescent field.
2. The application of chemometrics techniques such as partial least squares and principal component regression to construct the calibration model between infrared absorbance spectra and solution concentrations. These techniques can incorporate the effects of peak shifts into the calibration and automatically weigh more strongly the absorbances that are more highly predictive of the solution concentrations.
3. The inclusion of the temperature with the absorbances in the chemometric calibration. Earlier approaches for temperature compensation (21) had poor accuracy.
4. The use of a pure gas or liquid instead of laboratory air for collection of a background spectrum. Using laboratory air causes uncontrolled variations in the background spectrum, as the humidity of the air around a crystallizer is highly variable, and water strongly absorbs light within a wide range of the mid-infrared region of the spectrum. A stable background spectrum is obtained when using a pure liquid such as the solvent or dry nitrogen gas.

Accuracies as high as 0.00014 g solute/g solvent were reported by early 2002 (22); the achievable accuracy of the solution concentration measurement for a particular experiment varied depending on the infrared spectrometer, the ATR-FTIR probe, the particular solutes and solvents, and whether the above protocols were followed. A huge number of academic and industrial applications of ATR-FTIR spectroscopy quickly followed (23), including the demonstration of high accuracies for a pharmaceutical crystallizer at Merck with four components in solution (24).

Next-Generation Optimal Control Formulations for Crystallizers

As discussed in the introduction, the model-based optimal control formulations applied for decades to continuous crystallization had limitations in terms of optimization objectives and constraints,

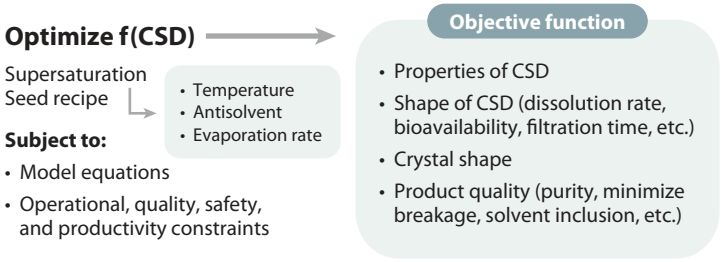

Figure 1

Generic formulation of the model-based crystallization control approach as an optimization problem that indicates the typical optimization objectives, optimization variables, and constraints (31). Abbreviation: CSD, crystal size distribution. Figure adapted from Reference 31.

optimization variables, and methods of dealing with uncertainties. These limitations have been removed in the past 10–15 years, and many extensions have been developed to consider new crystal product quality characteristics and optimization variables (**Figure 1**). The optimization is subject to the model equations and various constraints owing to equipment limitations (e.g., maximum and minimum temperature values, maximum and minimum cooling rates, maximum volume, limits on antisolvent addition rate), productivity requirements (to ensure a desired yield at the end of the batch), and quality specifications (e.g., 2, 25–28). Usually the optimization objectives such as the number-average crystal size, coefficient of variation, nucleated-to-seed-mass ratio, and weight-mean size can be computed efficiently using the method of moments (29), but the optimal operating conditions and their robustness may depend strongly on the objective (4, 9–12, 30–32).

A major advance in the application of model-based control approaches is the development of comprehensive uncertainty analysis and robust optimization formulations that are able to account for the effects of realistic uncertainties and disturbances on optimal operating policies. Uncertainties in the model parameters or structure or in the recipe or control implementation should be carefully assessed using robustness analysis techniques (10, 30, 32, 33), and if the effects of these uncertainties are significant, they should be taken into account in the optimization. Robust optimization approaches include the optimization of the worst-case objective as well as a weighted sum of the mean of the objective and its variance owing to uncertainties. The latter is a multiobjective optimization that allows tailoring of the trade-off between nominal performance and robustness and has been used successfully for robust control of the crystal size distribution (CSD) (11, 12, 15) and the polymorphic form (34) (polymorphic crystals contain the same molecular species but have different packing of molecules within the crystal structure). A distribution shaping control (DSC) allows the precise tailoring of the shape of the CSD, which enables the implementation of a product engineering approach to control the crystallization process to directly achieve the desired final product quality (15, 35–37). The optimization objective for DSC can be formulated directly in terms of the CSD or using the quantiles of the cumulative distribution. Increased robust performance can be achieved by repeating the optimization on-line on the basis of real-time measurements and state estimation, which is known in the literature as model predictive control (11, 15, 38–40). The supersaturation trajectory can be optimized directly in the crystallization phase diagram and implemented using concentration feedback control (CFC) (also known as supersaturation control) approaches in a hierarchical structure (15), or can be optimized in the time domain using the actual manipulated variables used to generate the supersaturation (e.g., temperature, antisolvent addition profile, evaporation rate). The advantages of combining the supersaturation generation methods by simultaneously optimizing cooling and antisolvent addition to achieve

CSD: crystal size distribution

Polymorphs: different crystal structures of the same molecule

CFC: concentration feedback control; synonymous with supersaturation control

Supersaturation control: synonymous with concentration feedback control (CFC)

larger and more uniform crystals have been demonstrated (41, 42). Better control over the shape of the final CSD can be obtained by allowing controlled dissolution of the fine particles by including the dissolution mechanisms in the model (43) or/and by the simultaneous optimization of the seeding (4, 5, 44–46) with the operating curve. Just as is the case for manipulated variable profiles (10), variations in the seed quality can cause drastic variations in the product quality (6).

Development of Sensors and Models for Crystal Shape

The monitoring and control of crystal shape has received significant attention in recent years. Image analysis is a direct observation method that is used mainly for the classification of crystals on the basis of their size or morphology. Images can be acquired from outside of the crystallizer through an observation window (47, 48) or by using high-resolution in situ video microscopy tools such as the Mettler-Toledo Particle Vision Microscope or similar systems (1, 22, 38, 49–54). Methods based on low-resolution cameras (bulk video imaging) have also been used to detect nucleation and polymorphic transformation (55–58); however, these approaches are not suitable for quantitative determination of shape and size distribution. The aforementioned techniques are able to extract 2D shape and size information. Newer methodologies based on digital holography can extract 3D information from specially acquired images (59, 60). A major limitation of most approaches based on in situ image analysis is the low solid concentration for which the approaches provide quantitative results (typically a maximum of 5–7%). Future research will focus on developing new hardware and software systems that can provide reliable quantitative information at higher solid concentrations in the suspensions.

The dynamic evolution of the crystal shape is modeled using a multidimensional population balance equation, which considers the growth of particles in two or more characteristic dimensions (7, 29, 37, 61–67). The model requires the identification of growth kinetics in each characteristic length (68), which can be determined on the basis of size and shape information obtained from the imaging tools. The evolution of crystal shape considering both growth and dissolution mechanisms has also been modeled; this work together with other experimental investigations indicates that dissolution cycles can provide an additional degree of freedom to control the particle shape and size (69–73).

Robust Concentration Feedback Control

The availability of accurate in situ concentration measurement tools based on ATR-FTIR or ATR-UV/Vis spectroscopy coupled with robust chemometrics approaches has enabled the application of CFC approaches to both cooling and antisolvent crystallization systems at laboratory as well as industrial scales. The benefits of CFC (with some variations in the implementation) to achieve improved product properties (larger and more uniform crystals with less agglomeration) have been extensively reported in the literature (14, 16, 22, 74–79). The CFC approach is based on the fundamental understanding of the crystallization operation within the phase diagram between the solubility and metastable curves. Often an absolute or relative supersaturation set point is specified so the term "supersaturation control" is often used to describe the method in the literature, but this is actually a misnomer because a solute concentration rather than a supersaturation is directly measured. The approach can be used to specify an arbitrary concentration target profile in the phase diagram; this can be particularly useful for the control of polymorphic crystallization processes in which more complex trajectories may be needed for the selective control of a particular polymorphic or pseudopolymorphic form (80, 81) (pseudopolymorphic crystals have different incorporation of solvent molecules into their crystal structures). For typical batch cooling crystallization processes, the controller calculates the supersaturation using real-time concentration $C(t)$

Pseudopolymorphs: crystal structures that have different incorporation of solvent molecules within their crystal lattices; also referred to as solvates or solvatomorphs

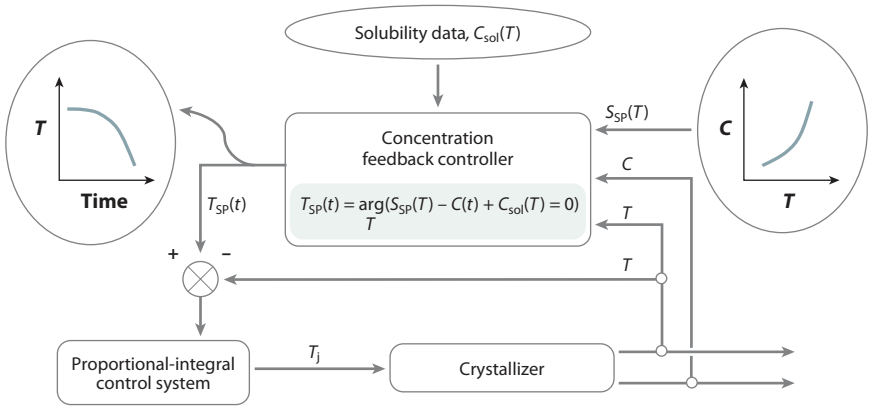

Figure 2

Generic block diagram of the concentration feedback or supersaturation control approach. Abbreviations: *C*, concentration, C_{sol}, saturation concentration (solubility); j, jacket; *S*, absolute supersaturation; SP, set point; *T*, temperature; *t*, time.

and temperature $T(t)$ measurements, as well as the solubility $C_{sol}(T)$, and adjusts the temperature to maintain or follow the desired target supersaturation $S_{SP}(T)$ in the phase diagram (**Figure 2**). The calculated temperature set point $T_{SP}(t)$ is sent to the lower-level temperature controller [typically a cascade proportional-integral (PI) control system]. This approach has the advantage that, by specifying the operating trajectory in the crystallization phase diagram, a nearly optimal operating curve in the time domain (e.g., temperature profile) is automatically determined, which then can be implemented directly at the production scale using a standard tracking control system (direct design approach) (14). This approach provides a model-free (direct design) alternative to the programmed cooling approach that determines the optimal temperature trajectory corresponding to a particular constant supersaturation by using a simple mathematical description of the kinetic processes involved in the crystallization (82). **Figure 3*a*** shows an example of supersaturation and the resulting temperature trajectories obtained by the implementation of CFC for the crystallization of paracetamol in isopropanol. The large uniform crystals obtained at the end of the batch are shown in **Figure 3*b***. The set point can be selected by using an automated system that runs multiple experiments and selects the operating conditions for which the crystals meet the product specifications (79) or by applying measurement-based optimization approaches according to a batch-to-batch iterative learning control framework (37, 41, 83–85). The supersaturation can be expressed in absolute or relative values or as a supersaturation ratio, and the approach applies similarly to antisolvent crystallization systems. The approach can be extended to combined cooling and antisolvent crystallization by expressing the solubility and the set point trajectory as functions of both the temperature and the solvent composition.

Sensors, Models, and Robust Control of Polymorphic and Pseudopolymorphic Forms

Polymorphic crystals contain the same molecular species but have different packing of molecules within the crystal structure, whereas pseudopolymorphic crystals have the same primary molecular species but different incorporation of solvent molecules within the crystal structure. Manufacturing the desired crystal form is quite important in the pharmaceutical industry, as different forms can have rather different physical properties, such as solubility, dissolution rate, and shape (e.g., **Figure 4*a–c***), and hence different effects on the biological organism.

PI: proportional-integral

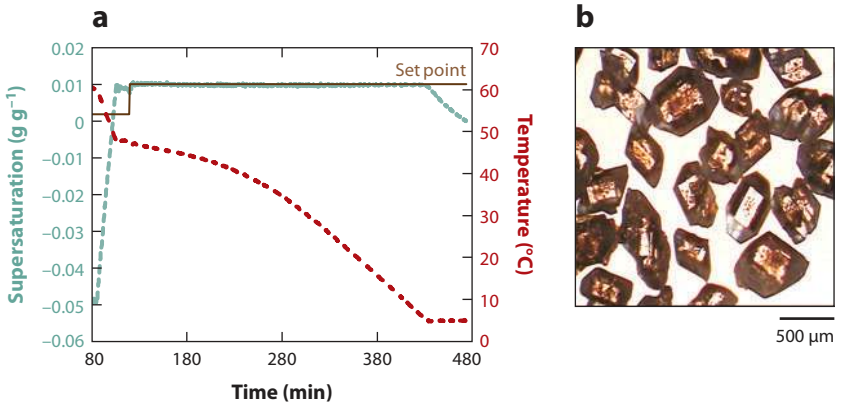

Figure 3

(*a*) Supersaturation and corresponding temperature profiles obtained during the concentration feedback control (CFC) of paracetamol in isopropanol. The feedback controller is able to track the desired constant supersaturation, and the controller automatically generates the temperature versus time trajectory. (*b*) Micrograph of the product crystals obtained using CFC that indicate large uniform crystals and no agglomeration. Figure adapted from Reference 122.

Several sensors for monitoring multiple crystal forms during crystallization have been developed in the last 10–20 years, including Raman spectroscopy (86–88), in situ X-ray diffraction (89), in situ laser backscattering (90, 91), and in situ process video microscopy. Although none of these sensors provides sufficient accuracy for model development for all solute-solvent systems, for most systems at least one of these sensor technologies can be used to monitor the transformation between different crystal forms (92, 93). In recent years these sensors have been used to construct rather detailed population balance models that describe such transformations (54, 94–99) and have been used to compare the closed-loop performance of a wide variety of advanced control strategies (34, 83, 84, 100). The generation of large crystals of a desired form, even for highly metastable crystals, has been experimentally demonstrated without use of surfactants or other additives for stabilization (80, 81) by employing the robust CFC strategy described in the Robust Concentration Feedback Control section (**Figure 4*c,d***).

Development of Microfluidic Crystallization Platforms for Crystallization Modeling and Control

A major advance in crystallization technology over the past decade has been the development of microfluidic crystallization platforms (101–104). These enable the high-throughput search for polymorphic and pseudopolymorphic forms and the selection of solvents that maximize molecular purity and yield while enabling the manufacture of the desired form using tiny amounts of material (typically, a protein or pharmaceutical). Most of these technologies employ droplets with volumes in the nano- to microliter range; the nucleation-related measurement is the induction time, which is the time required to nucleate a crystal in a supersaturated solution. A recent advance is the development of methods for using such platforms for the determination of primary nucleation kinetics at supersaturations that are too high to be obtainable in larger-scale crystallizations. Many companies have proposed crystallizer designs that operate at high supersaturation to nucleate seed crystals that are subsequently grown to a desired size (105–108). These kinetics are required in crystallization simulations for use in the evaluation of crystallizer design and control strategies (e.g., References 109, 110, and references therein).

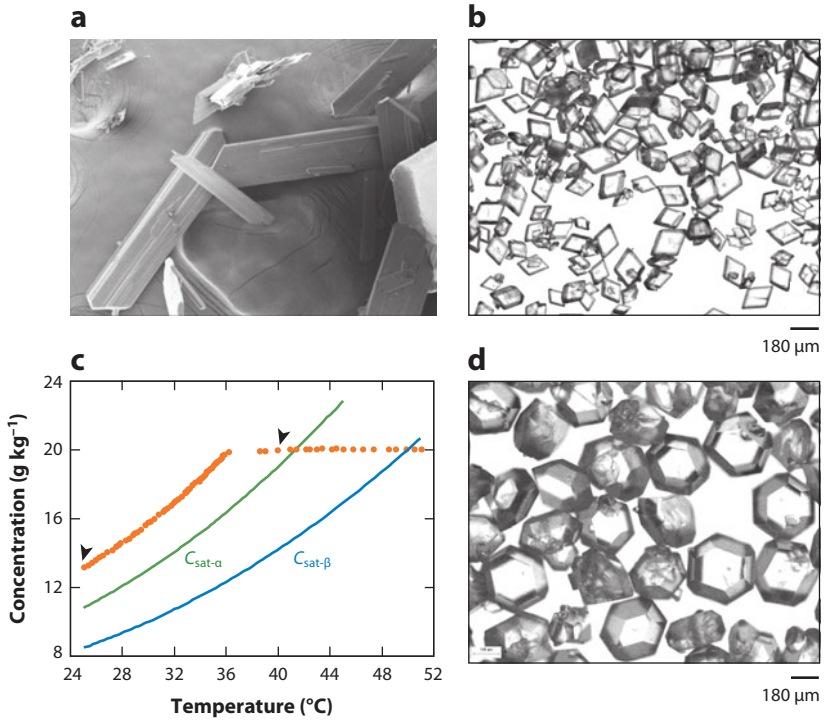

Figure 4

(*a*) Stable β-form crystals of L-glutamic acid, (*b*) metastable α-form seed crystals of L-glutamic acid (100–300 μm), (*c*) controlled path (*orange dots*) in the crystallization phase diagram with seeding point and end point shown with arrowheads, and (*d*) product crystals (330–600 μm). No stable β-form crystals were observed in the product using either off-line X-ray diffraction or optical microscopy. The β-form crystals are elongated plates of high aspect ratio. Figure adapted from Reference 81.

The measurement of nucleation kinetics at the microscale is quite different than that in macroscale crystallizers, as the induction time is highly stochastic owing to the small volumes and the inherent stochasticity of molecular events. In particular, the induction time for a particular solute and solvents can vary by as much as a factor of two even when two droplets operate under exactly the same supersaturation trajectory over time. Modeling the relationship between the nucleation kinetics and the measured induction times requires a stochastic model that is most naturally written in the form of a chemical master equation (e.g., 111). An analytical solution for this equation for arbitrary supersaturation trajectories was recently derived (112–114) that enables the nucleation kinetics to be estimated in a wide range of droplet and microfluidics-based devices, including levitated droplet systems (115), continuous flow plug-based crystallization (116), and patterned substrate-based systems (117). Such applications have been demonstrated for several solute-solvent systems (112).

PROMISING RESEARCH DIRECTIONS

Robust Model-Free Control of Crystallizers

Most crystallization control approaches restrict the operation within the metastable zone. Although this approach is effective for most pharmaceutical crystallizations, it can be sensitive

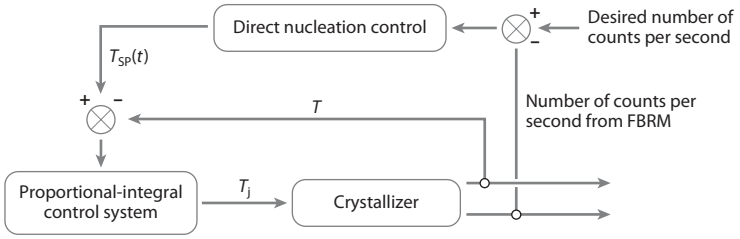

Figure 5

Schematic block diagram of the direct nucleation control for batch cooling crystallization processes. Abbreviations: FBRM, focused beam reflectance measurement; j, jacket; SP, set point; *T*, temperature; *t*, time.

to accidental seeding, attrition of very brittle crystals, significant variations in seed quality, or large variations in the metastable limit or solubility owing to variations in the contaminant profile of the feed streams. Several model-free approaches have been proposed to robustly control such crystallizations that allow a controlled crossing of the boundaries of the metastable zone and drive the crystallization operations into the undersaturated region (118). The direct nucleation control (DNC) approach (85) maintains the number of particles at a predetermined value during the crystallization and is based on the idea that the lower the number of crystals is in the system, the larger the size of the product crystals. The number of crystals is measured in situ using focused beam reflectance measurement (FBRM), although other measurement techniques that provide a signal that is a continuous function of the number of crystals (such as turbidity, bulk video imaging, and ultrasonic attenuation) could be employed. Correlations between the number of counts per second provided by the FBRM and the size of the crystals can be obtained off-line, and the DNC approach can be used to indirectly control product properties. The target number of counts per second is controlled by successive supersaturation generation (e.g., by cooling or antisolvent addition) and dissolution phases (e.g., by heating or solvent addition).

The cooling/heating or antisolvent/solvent addition rates can be predetermined, or for more accurate control they can be functions of the difference between the measured and target counts per second (**Figure 5**). The benefits of the DNC approach have been demonstrated for the production of crystals with desired mean size (118–119), reduction of solvent inclusion (120), achievement of better polymorphic purity (73), and improvement of the surface properties of the crystals (72). A typical time-domain operating profile with the characteristic automatically determined heating-cooling cycles in the case of the unseeded cooling crystallization of paracetamol in isopropanol is shown in **Figure 6*a***. The corresponding crystallization phase diagram with the automatic dissolution loops is shown in **Figure 6*b***. The crystals produced at the end of the DNC experiments are significantly larger, more uniform in size, and less agglomerated compared with the product obtained using linear cooling (**Figure 6*c*,*d***).

The DNC approach is a completely adaptive and quite robust methodology for crystallization scale-up that requires virtually no prior information about the model, kinetics, or metastable zone width of the crystallization process (121, 122), because both the solubility and nucleation curves are detected automatically during the control. The method automatically adapts the operating conditions when changes are detected in the measured number of crystals; hence, it is highly robust to variations in the seed quality (e.g., initial breeding) or addition point (i.e., partial dissolution or secondary nucleation because of too early or too late addition) as well as to accidental seeding from crust.

To reduce the number of dissolution cycles (and thus the batch time) resulting from the initial implementation of the DNC approach, measurement-based optimization approaches can

DNC: direct nucleation control

FBRM: focused beam reflectance measurement

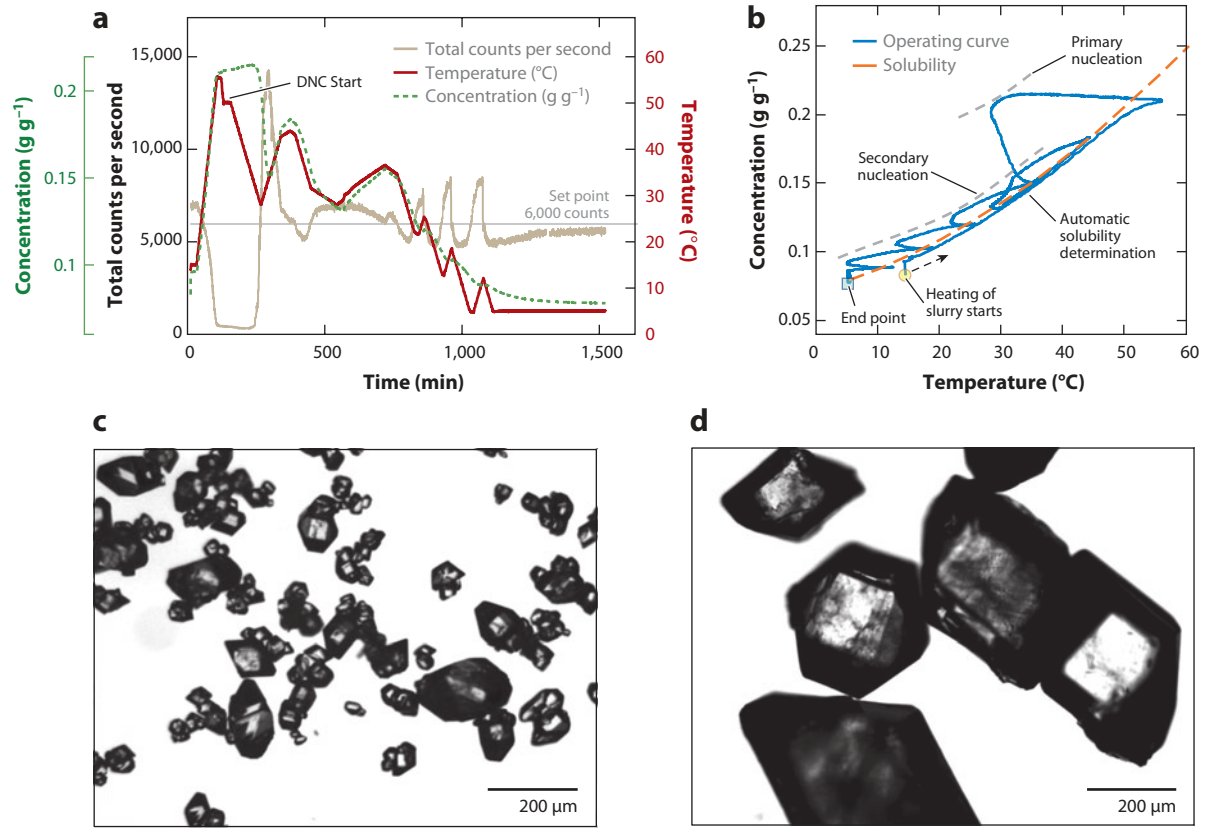

Figure 6

(*a*) Temperature, focused beam reflectance measurement (FBRM) counts per second, and concentration profiles over time during a typical direct nucleation control (DNC) experiment with paracetamol in isopropanol at a target of 6,000 counts s^{-1}. (*b*) Corresponding operating curve in the crystallization phase diagram indicating the series of nucleation events (the first nucleation occurs at a much larger supersaturation) and the dissolution loops corresponding to the heating-cooling phases in panel *a*. (*c*) Micrograph of product crystals from a typical unseeded linear cooling experiment indicating small agglomerated crystals. (*d*) Micrograph of product crystals from the experiment using the DNC approach; these crystals are significantly larger with more uniform size and no agglomeration. Figure adapted from Reference 122.

be applied on the basis of an iterative learning control framework, which uses information from previous batches to improve the operating profile of the subsequent batch in a combined feedforward–feedback control architecture (37, 83, 84). Alternatively, CFC and DNC approaches can be used in combination either simultaneously or sequentially. In the simultaneous approach, CFC and DNC are applied in a hierarchical structure in which the process is controlled mainly within the metastable zone by the supersaturation controller. The direct nucleation controller reacts when changes in the number of crystals are detected by adapting the set point of the supersaturation controller. The sequential approach uses first the DNC approach for in situ seed generation via primary nucleation and controlled dissolution of the excess crystals. When the desired number of counts per second is achieved, the approach switches to CFC, which controls the crystallization process in the phase diagram at a predetermined supersaturation level. The DNC approach also can be applied to continuous crystallization systems by creating the dissolution loops spatially by generating alternating supersaturated and

undersaturated zones (by cooling/heating or multiple injections of antisolvent or solvent) along the reactor.

New Crystallizer Designs

Many new designs for crystallizers have been developed in recent years; in some cases these pose control challenges, and in other cases they open up new opportunities for feedback control. For example, a proposed continuous oscillatory baffled crystallizer employs a piston to agitate the crystal slurry in a long pipe with baffles (123). Such a crystallizer typically can operate at lower shear rates than a single stirred-tank crystallizer, but it is limited to lower solid densities and effective viscosities and has limited degrees of freedom for feedback control. Several continuous tubular crystallizers have been investigated (e.g., 124), often with static mixers or baffles introduced to better emulate plug flow so as to obtain a narrower CSD, but the baffles or other constructions in the path of the flow applied to achieve the static mixing effect have the potential to cause fouling. Especially interesting from a control point of view is a tubular crystallizer design that introduces antisolvent at multiple points along the crystallizer (125), which provides many more degrees of freedom for feedback control compared with most alternative designs. A tubular crystallizer that is less prone to fouling and ensures plug-flow behavior segments the flow into liquid slugs separated by an immiscible fluid (126). The fluid in each liquid slug is well mixed as long as the length of the liquid slug is not much larger than the pipe diameter. A variation on this approach is to carry out the crystallization within droplets, which makes fouling nearly impossible and provides a higher surface area-to-volume ratio so that uniform control of temperature within each droplet is easy (e.g., 127, 128).

Most of these continuous-flow crystallizers are not specifically designed to provide many degrees of freedom for the control of crystal size, shape, and polymorphic identity in the presence of process disturbances and variations in crystallization kinetics owing to changes in the contaminant profile. A semicontinuous crystallization configuration has been proposed that combines a small crystallizer for continuous seed generation with a downstream large stirred-tank crystallizer operated using the robust CFC method (described in the Robust Concentration Feedback Control section) to minimize nucleation and promote crystal growth (129). The extra degrees of freedom that come from having independent continuous control of nucleation in one crystallizer and control of growth in a separate crystallizer results in a high degree of CSD controllability. This approach was demonstrated experimentally for a flat-top CSD that cannot be achieved in a standard crystallizer; the measured CSD was quite close to that predicted by theory (130). Many of these same control principles and controller design methods should be incorporated into other continuous flow crystallizer designs; otherwise, it may become impossible to reliably achieve the desired crystal product at industrial manufacturing scale.

Simultaneous Control of Shape and Crystal Size Distribution by Robust Crystallization Path Design

Simultaneous robust control of several crystal properties (e.g., size, shape, polymorphic form) has become increasingly important with the continuously tightening regulatory constraints on product properties. Several control approaches, both within-batch and batch-to-batch, have been proposed for the simultaneous control of shape and CSD (36, 37, 131). This simultaneous control can be achieved by formulating a model-based robust distribution shaping control problem that also incorporates constraints on the crystal shape (37),

$$\min_{C_{\mathrm{SP},k}(u)} \left\{ (1-w) \sum_i \left[f(r_i, t_f; \hat{\theta}_k) - f^{\mathrm{target}}(r_i) \right]^2 + wV\left[f(r_i, t_f; \theta_k) \right] \right\}, \qquad 1.$$

subject to the model equations and the constraints,

$$u_{\min}(k) \le u(k) \le u_{\max}(k), \quad 2.$$

$$R_{\min}(k) \le \frac{\mathrm{d}u(k)}{\mathrm{d}t} \le R_{\max}(k), \quad 3.$$

$$C(t_f) \le C_{f,\max}, \quad 4.$$

$$\beta_{\min} \le \beta \le \beta_{\max}, \quad 5.$$

where $f(r_i, t_f; \hat{\theta}_k)$ and $f^{\text{target}}(r_i)$ are the simulated (at the end of the batch) and the target numbers of crystals in the discretized size interval i; $V[f(r_i, t_f; \theta_k)]$ is the variance of the predicted number of crystals in the size interval i owing to parametric uncertainties in the model; $C_{\text{SP},k}(u)$ is the operating curve in the phase diagram $C - u$ in batch k, which is used as the set point for the supersaturation controller; and $w \in (0, 1)$ weights the relative importance of nominal product quality and robustness to model uncertainties. The variable u denotes the temperature ($u = T$) for cooling crystallization and the solvent concentration in the case of antisolvent crystallization systems. The duration of the batch is t_f, and $u_{\min}$, $u_{\max}$, $R_{\min}$, and $R_{\max}$ are the minimum and maximum temperatures or antisolvent addition flow and their changing rates, respectively, during the batch. The objective function can be based on the cross-moments, on the 2D CSD directly (7), or on a 1D CSD, as shown in Equation 1, which can be computed using the equivalent spherical diameter (r). In all cases, the process model is expressed by a multidimensional population balance model. The constraints in Equations 1 and 2 ensure that the temperature profile stays within the operating range of the crystallizer. The constraint in Equation 4 ensures that the solute concentration at the end of the batch, $C(t_f)$, is smaller than a certain maximum value, $C_{f,\max}$, set by the minimum yield required by economic considerations. The last constraint restricts the aspect ratio, expressed as the ratio between two characteristic sizes of the crystals ($\beta = L_1/L_2$), to be between desired minimum ($\beta_{\min}$) and maximum ($\beta_{\max}$) values.

The approach can be implemented as the three-level hierarchical control shown in **Figure 7** (15, 31), in which the level-3 model-based control repeatedly optimizes the operating trajectory defined in the crystallization phase diagram, which is used as the set point for a level-2 concentration feedback controller that manipulates the set point of a level-1 temperature controller (simple or cascade PI controller) to follow the desired concentration trajectory in the phase diagram.

The approach that determines operating profiles in the crystallization phase diagram provides a much more intuitive framework for defining the design and control space and allows the use of significantly simpler models in model-based optimization and control. This is especially true in the case of polymorphic systems, in which setting constraints that directly restrict the operating trajectory to be within the region of the phase diagram where a particular polymorph is stable can eliminate the need to model the potential polymorphic transformation, which is required for optimization of the operating trajectory parameterized in the time domain (34, 84, 100). Similarly, nucleation can be avoided simply by directly setting the appropriate bounds on the set point trajectory without necessarily needing to model (and identify) nucleation kinetics, whereas the similar constraint when the optimization is performed in the time domain can be implemented only indirectly.

The control of crystal shape and of the CSD are highly correlated, which can significantly limit the achievable combinations (37). Molecular additives can be introduced into the system in low quantities to provide an additional manipulated input for better crystal shape control (132). These additives can have strong and selective effects on the nucleation or growth rates of different crystal faces (46, 133, 134) and can be used as an additional manipulated input to decouple the control of CSD and shape.

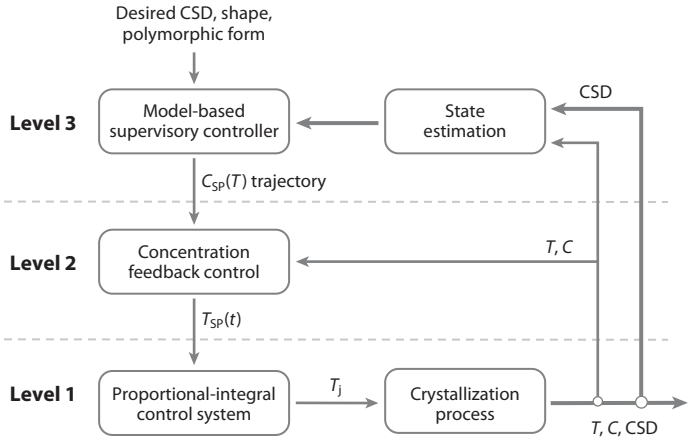

Figure 7

Block diagram of the three-level hierarchical nonlinear model predictive control system for crystallization processes. The high-level (level 3) supervisory controller optimizes the operating trajectory in the crystallization phase diagram. The optimal trajectory is sent to the level 2 concentration feedback controller that tracks the profile in the phase diagram by manipulating the jacket temperature T_j through the low-level (level 1) temperature proportional-integral control system. Abbreviations: *C*, concentration; CSD, crystal size distribution; j, jacket; SP, set point; *T*, temperature; *t*, time. Figure adapted from Reference 31.

Interconnected Crystallization Systems for Multicomponent Crystallization

The availability of ATR spectroscopy coupled with robust multivariate statistical approaches has enabled the simultaneous monitoring of multiple components during crystallization (24). This availability allows the control of the trajectories of multiple species in the crystallization phase diagram so that crystallization control approaches can be applied to multicomponent systems. This control can be achieved by interconnected crystallization systems that allow the transfer of the liquid phase only, which can be achieved by circulation of the filtered liquid between vessels or by separation of the crystallization cells using membranes permeable to the liquid only. Each crystallizer/compartment is seeded with one particular component of the mixture, and supersaturation is generated in the entire system by cooling, antisolvent addition, or evaporation. The components will grow preferentially in the compartments with the corresponding seed, but the concentrations of all species decrease simultaneously in all compartments, thus avoiding cross contamination owing to heterogeneous nucleation of the other components. Two coupled crystallization systems have been used for the separation of enantiomers (135–138). The concept was also applied successfully to the separation of the positional isomers (*ortho*, *meta*, and *para*) of aminobenzoic acid in a system consisting of three interconnected crystallizers (139). The approach can be extended to an arbitrarily large number of components, for example, by developing a matrix of crystallization cells separated by membranes permeable to the liquid only. These interconnected systems can be operated in both batch and continuous mode. Certain limitations of the approach may exist for systems with complex phase diagrams (e.g., systems with eutectics) or if the components may form cocrystals.

Composite Sensor Arrays and the Crystallization Process Informatics System

The recent development of in situ sensors with process analytical technologies (PATs) has led to the widespread application of various measurement techniques. These instruments are often used

PAT: process analytical technology

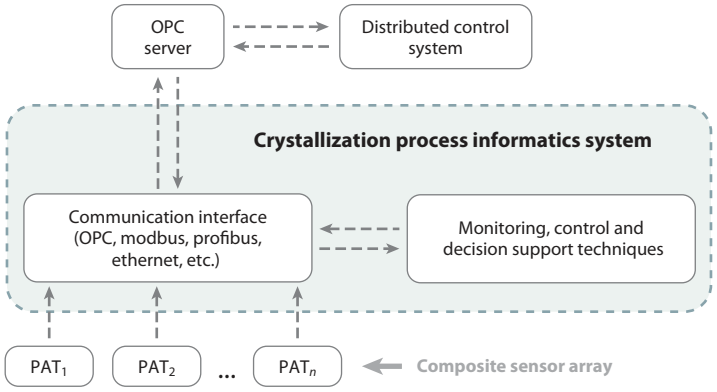

Figure 8

Schematic representation of the architecture of the crystallization process informatics system with an industry standard communication interface with the composite sensor array and the distributed control system. Abbreviations: OPC, object linking and embedding for process control; PAT, process analytical technology. Figure adapted from Reference 31.

simultaneously to monitor crystallization processes; however, the information that is provided is seldom combined and applied in real time. More recently, the concept of a composite sensor array (CSA) has been introduced, which is based on the idea that all instruments are considered to be components of a single global sensor that provides various signals from the crystallization process. These are then analyzed simultaneously using model-based approaches or by applying chemometrics techniques (e.g., those based on principal component analysis) with a system that automatically determines the most relevant combination of signals for a particular process or control objective. The complementarity and redundancy in the acquired information allow the implementation of robust crystallization control strategies. The various components of the CSA are coordinated by a crystallization process informatics system (CryPRINS) (140) that monitors multiple process and quality properties at the same time and simultaneously uses all signals from all measurement devices for automated decision support and feedback control of the crystallization process (**Figure 8**). To become readily applicable in an industrial environment, such a system (e.g., CryPRINS) must provide a generic communication interface based on industrial standard protocols such as OPC [object linking and embedding (OLE) for process control] or modbus that allows the communication between the various PATs provided by different vendors and the distributed control system (DCS) necessary to implement the proposed control actions.

DISCLOSURE STATEMENT

The authors are not aware of any affiliations, memberships, funding, or financial holdings that might be perceived as affecting the objectivity of this review.

CSA: composite sensor array

CryPRINS: crystallization process informatics system

ACKNOWLEDGMENTS

Nicholas Kee at ExxonMobil is acknowledged for the preparation of **Figure 4** and Mo Jiang, Zhilong (Peter) Zhu, and Lifang Zhou at the Massachusetts Institute of Technology are acknowledged for discussions on next-generation continuous-flow crystallizer designs. Ali Saleemi and Rushdi Abu Bakar from Loughborough University, UK, are acknowledged for producing the experimental results using the CFC and DNC approaches. Financial support is acknowledged

by the Process Systems Engineering Consortium and the European Research Council under the European Union's Seventh Framework Program (FP7/2007–2013)/ERC grant agreement no. [280106-CrySys].

LITERATURE CITED

1. Braatz RD. 2002. Advanced control of crystallization processes. *Annu. Rev. Control* 26:87–99
2. Rawlings JB, Miller SM, Witkowski WR. 1993. Model identification and control of solution crystallization processes: a review. *Ind. Eng. Chem. Res.* 32:1275–96
3. Braatz RD, Fujiwara M, Ma DL, Togkalidou T, Tafti DK. 2002. Simulation and new sensor technologies for industrial crystallization: a review. *Int. J. Mod. Phys. B* 16:346–53
4. Chung SH, Ma DL, Braatz RD. 1999. Optimal seeding in batch crystallization. *Can. J. Chem. Eng.* 77:590–96
5. Aamir E, Nagy ZK, Rielly CD. 2010. Optimal seed recipe design for crystal size distribution control for batch cooling crystallization processes. *Chem. Eng. Sci.* 65:3602–14
6. Aamir E, Nagy ZK, Rielly CD. 2010. Evaluation of the effect of seed preparation method on the product crystal size distribution for batch cooling crystallization processes. *Cryst. Growth Des.* 10:4728–40
7. Ma DL, Tafti DK, Braatz RD. 2002. Optimal control and simulation of multidimensional crystallization processes. *Comput. Chem. Eng.* 26:1103–16
8. Ma DL, Braatz RD. 2003. Robust identification and control of batch processes. *Comput. Chem. Eng.* 27:1175–84
9. Ward JD, Mellichamp DA, Doherty MF. 2006. Choosing an operating policy for seeded batch crystallization. *AIChE J.* 52:2046–54
10. Nagy ZK, Braatz RD. 2003. Worst-case and distributional robustness analysis of finite-time control trajectories for nonlinear distributed parameter systems. *IEEE Trans. Control Syst. Technol.* 11: 694–704
11. Nagy ZK, Braatz RD. 2003. Robust nonlinear model predictive control of batch processes. *AIChE J.* 49:1776–86
12. Nagy ZK, Braatz RD. 2004. Open-loop and closed-loop robust optimal control of batch processes using distributional and worst-case analysis. *J. Process Control* 14:411–22
13. Nagy ZK, Fujiwara M, Woo XY, Braatz RD. 2008. Determination of the kinetic parameters for the crystallization of paracetamol from water using metastable zone width experiments. *Ind. Eng. Chem. Res.* 47:1245–52
14. Fujiwara M, Nagy ZK, Chew JW, Braatz RD. 2005. First-principles and direct design approaches for the control of pharmaceutical crystallization. *J. Process Control* 15:493–504
15. Nagy ZK. 2009. Model based robust control approach for batch crystallization product design. *Comput. Chem. Eng.* 33:1685–91
16. Nagy ZK, Chew JW, Fujiwara M, Braatz RD. 2008. Comparative performance of concentration and temperature controlled crystallizations. *J. Process Control* 18:399–407
17. **Dunuwila DD, Carroll LB, Berglund KA. 1994. An investigation of the applicability of attenuated total-reflection infrared-spectroscopy for measurement of solubility and supersaturation of aqueous citric acid solutions. *J. Cryst. Growth* 137:561–88**
18. Dunuwila DD, Berglund KA. 1997. ATR FTIR spectroscopy for in situ measurement of supersaturation. *J. Cryst. Growth* 179:185–93
19. Barnes HA. 1995. A review of the slip (wall depletion) of polymer solutions, emulsions and particle suspensions in viscometers: its cause, character, and cure. *J. Non-Newton. Fluid* 56:221–51
20. Togkalidou T, Fujiwara M, Patel S, Braatz RD. 2001. Solute concentration prediction using chemometrics and ATR-FTIR spectroscopy. *J. Cryst. Growth* 231:534–43
21. Lewiner F, Klein JP, Puel F, Févotte G. 2001. On-line ATR FTIR measurement of supersaturation during solution crystallization processes. Calibration and applications on three solute/solvent systems. *Chem. Eng. Sci.* 56:2069–84

17. Demonstrated ATR-FTIR spectroscopy for measurement of a solute concentration during a solution crystallization.

22. Fujiwara M, Chow PS, Ma DL, Braatz RD. 2002. Paracetamol crystallization using laser backscattering and ATR-FTIR spectroscopy: metastability, agglomeration and control. *Cryst. Growth Des.* 2:363–70

23. An overview of early crystallization control technology from the U.S. Food and Drug Administration.

23. Yu LX, Lionberger RA, Raw AS, D'Costa R, Wu H, Hussain AS. 2003. Applications of process analytical technology to crystallization processes. *Adv. Drug Deliv. Rev.* 56:349–69

24. Togkalidou T, Tung HH, Sun YK, Andrews A, Braatz RD. 2002. Solution concentration prediction for pharmaceutical crystallization processes using robust chemometrics and ATR FTIR spectroscopy. *Org. Process Res. Dev.* 6:317–22

25. Worlitschek J, Mazzotti M. 2004. Model-based optimization of particle size distribution in batch-cooling crystallization of paracetamol. *Cryst. Growth Des.* 4:891–903

26. Corriou JP, Rohani S. 2008. A new look at optimal control of a batch crystallizer. *AIChE J.* 54:3188–206

27. Sarkar D, Rohani S, Jutan A. 2006. Multi-objective optimization of seeded batch crystallization processes. *Chem. Eng. Sci.* 61:5282–95

28. An overview of crystallization process control up to 2005.

28. Larsen PA, Patience DB, Rawlings JB. 2006. Industrial crystallization process control. *IEEE Control Syst. Mag.* 26(4):70–80

29. Hulbert HM, Katz S. 1964. Some problems in particle technology. *Chem. Eng. Sci.* 19:555–74

30. Ma DL, Chung SH, Braatz RD. 1999. Worst-case performance analysis of optimal batch control trajectories. *AIChE J.* 45:1469–76

31. Nagy ZK, Braatz RD. 2012. Monitoring and advanced control of crystallisation processes. In *The Handbook of Industrial Crystallization*, ed. A Myerson, D Erdemir, A Lee. Cambridge: Cambridge Univ. Press. In press

32. Ma DL, Braatz RD. 2001. Worst-case analysis of finite-time control policies. *IEEE Trans. Contr. Syst. Technol.* 9:766–74

33. Matthews HB. 1997. *Identification and control of batch crystallization for an industrial chemical system*. PhD thesis. Univ. Wisc., Madison

34. Hermanto MW, Chiu MS, Woo XY, Braatz RD. 2007. Robust optimal control of polymorphic transformation in batch crystallization. *AIChE J.* 53:2643–50

35. Aamir E, Nagy ZK, Rielly CD, Kleinert T, Judat B. 2009. Combined quadrature method of moments and method of characteristics approach for efficient solution of population balance models for dynamic modelling and crystal size distribution control of crystallization processes. *Ind. Eng. Chem. Res.* 48:8575–84

36. Rusli E, Lee JH, Braatz RD. 2006. Optimal distributional control of crystal size and shape. *Proc. World Cong. Part. Technol., 5th, Orlando, FL*, Apr. 21-23, paper 240f. New York: AIChE Press. **http://aicheproceedings.org/**

37. Nagy ZK. 2009. Model based robust batch-to-batch control of particle size and shape in pharmaceutical crystallization. *Proc. Int. Fed. Autom. Contr. Symp. Adv. Contr. Chem. Process., 9th, Istanbul, Turkey*, July 12–15, pp. 200–5. Istanbul, Turkey: Koç Univ.

38. Larsen PA, Rawlings JB, Ferrier NJ. 2006. An algorithm for analyzing noisy, in situ images of high-aspect-ratio crystals to monitor particle size distribution. *Chem. Eng. Sci.* 61:5236–48

39. Mesbah A, Huesman AEM, Kramer HJM, Nagy ZK, Van den Hof PMJ. 2011. Real-time control of industrial batch crystallization processes using a population balance modeling framework. *AIChE J.* 57:1557–69

40. Mesbah A, Nagy ZK, Huesman AEM, Kramer HJM, Van den Hof PMJ. 2012. Real-time control of industrial batch crystallization processes using a population balance modeling framework. *IEEE Trans. Control Syst. Technol.* In press

41. Nagy ZK, Fujiwara M, Braatz RD. 2008. Modelling and control of combined cooling and antisolvent crystallization processes. *J. Process Control* 18:856–64

42. Lindenberg C, Krattli M, Cornel J, Mazzotti M, Brozio J. 2009. Design and optimization of a combined cooling/antisolvent crystallization process. *Cryst. Growth Des.* 9:1124–36

43. Nagy ZK, Aamir E, Rielly CD. 2011. Internal fines removal using a population balance model based control of crystal size distribution under dissolution, growth and nucleation mechanisms. *Cryst. Growth Des.* 11:2205–19

44. Doki N, Kubota N, Sato A, Yokota M. 2001. Effect of cooling mode on product crystal size in seeded batch crystallization of potassium alum. *Chem. Eng. J.* 81:313–16

45. Kalbasenka AN, Spierings LCP, Huesman AEM, Kramer HJM. 2007. Application of seeding as a process actuator in a model predictive control framework for fed-batch crystallization of ammonium sulphate. *Part. Part. Syst. Charact.* 24:40–48
46. Kubota N. 2001. Effect of impurities on the growth kinetics of crystals. *Cryst. Res. Technol.* 36:749–69
47. De Anda CJ, Wang XZ, Roberts KJ. 2005. Multi-scale segmentation image analysis for the in-process monitoring of particle shape with batch crystallisers. *Chem. Eng. Sci.* 60:1053–65
48. Dharmayat S, De Anda JC, Hammond RB, Lai XJ, Roberts KJ, Wang XZ. 2006. Polymorphic transformation of L-glutamic acid monitored using combined on-line video microscopy and X-ray diffraction. *J. Cryst. Growth* 294:35–40
49. Barrett P, Smith B, Worlitschek J, Bracken V, O'Sullivan B, O'Grady D. 2005. A review of the use of process analytical technology for the understanding and optimization of production batch crystallization processes. *Org. Process Res. Dev.* 9:348–55
50. Févotte G. 2002. New perspectives for the on-line monitoring of pharmaceutical crystallization processes using in situ infrared spectroscopy. *Int. J. Pharm.* 241:263–78
51. Kempkes M, Eggers J, Mazzotti M. 2008. Measurement of particle size and shape by FBRM and in situ microscopy. *Chem. Eng. Sci.* 63:4656–75
52. Larsen PA, Rawlings JB, Ferrier NJ. 2007. Model-based object recognition to measure crystal size and shape distributions from in situ video images. *Chem. Eng. Sci.* 62:1430–41
53. Larsen PA, Rawlings JB. 2009. The potential of current high-resolution imaging-based particle size distribution measurements for crystallization monitoring. *AIChE J.* 55:896–905
54. Schöll J, Bonalumi D, Vicum L, Mazzotti M, Muller M. 2006. In situ monitoring and modeling of the solvent-mediated polymorphic transformation of L-glutamic acid. *Cryst. Growth Des.* 6:881–91
55. Simon LL, Nagy ZK, Hungerbuhler K. 2009. Comparison of external bulk video imaging with focused beam reflectance and ultra violet-visible spectroscopy for crystallization nucleation detection and metastable zone identification. *Chem. Eng. Sci.* 64:3344–51
56. Simon LL, Nagy ZK, Hungerbuhler K. 2009. Endoscopy-based in situ bulk video imaging of batch crystallization processes. *Org. Process Res. Dev.* 13:1254–61
57. Simon LL, Oucherif KA, Nagy ZK, Hungerbuhler K. 2010. Bulk video imaging based multivariate image analysis, process control chart and acoustic signal assisted nucleation detection. *Chem. Eng. Sci.* 65:4983–95
58. Simon LL, Oucherif KA, Nagy ZK, Hungerbuhler K. 2010. Histogram matching, hypothesis testing, and statistical control-chart-assisted nucleation detection using bulk video imaging for optimal switching between nucleation and seed conditioning steps. *Ind. Eng. Chem. Res.* 49:9932–44
59. Eggers J, Kempkes M, Mazzotti M. 2008. Measurement of size and shape distributions of particles through image analysis. *Chem. Eng. Sci.* 63:5513–21
60. Darakis E, Khanam T, Rajendran A, Kariwala V, Naughton TJ, Asundi AK. 2010. Microparticle characterization using digital holography. *Chem. Eng. Sci.* 65:1037–44
61. Ma DL, Tafti DK, Braatz RD. 2002. Compartmental modeling of multidimensional crystallization. *Int. J. Mod. Phys. B* 16:383–90
62. Ma DL, Tafti DK, Braatz RD. 2002. High resolution simulation of multidimensional crystal growth. *Ind. Eng. Chem. Res.* 41:6217–23
63. Puel F, Févotte G, Klein JP. 2003. Simulation and analysis of industrial crystallization processes through multidimensional population balance equations. Part 1: a resolution algorithm based on the method of classes. *Chem. Eng. Sci.* 58:3715–27
64. Gunawan R, Fusman I, Braatz RD. 2004. High resolution algorithms for multidimensional population balance equations. *AIChE J.* 50:2738–49
65. Gunawan R, Fusman I, Braatz RD. 2008. Parallel high-resolution finite volume simulation of particulate processes. *AIChE J.* 54:1449–58
66. Ma CY, Wang XZ, Roberts KJ. 2008. Morphological population balance for modeling crystal growth in face directions. *AIChE J.* 54:209–22
67. Wan J, Wang XZ, Ma CY. 2009. Particle shape manipulation and optimization in cooling crystallization involving multiple crystal morphological forms. *AIChE J.* 55:2049–61

68. Gunawan R, Ma DL, Fujiwara M, Braatz RD. 2002. Identification of kinetic parameters in multidimensional crystallization processes. *Int. J. Mod. Phys. B* 16:367–74
69. Snyder RC, Veesler S, Doherty MF. 2008. The evolution of crystal shape during dissolution: predictions and experiments. *Cryst. Growth Des.* 8:1100–1
70. Lovette MA, Muratore M, Doherty MF. 2012. Crystal shape modification through cycles of dissolution and growth: attainable regions and experimental validation. *AIChE J.* 58:1465–74
71. Jiang M, Zhou L, Zhu X, Molaro M, O'Grady D, et al. 2011. In-situ identification of two-dimensional growth and dissolution kinetics for rod-like crystals. *Proc. Int. Symp. Ind. Cryst.*, *18th*, *Zürich*, *Switzerland*, Sept. 13–16, pp. 413–14. Milano, Italy: Ass. Italiana di Ing. Chim. (AIDIC)
72. Abu Bakar MR, Nagy ZK, Rielly CD. 2010. Investigation of the effect of temperature cycling on surface features of sulfathiazole crystals during seeded batch cooling crystallization. *Cryst. Growth Des.* 10:3892–900
73. Abu Bakar MR, Nagy ZK, Rielly CD. 2009. Seeded batch cooling crystallization with temperature cycling for the control of size uniformity and polymorphic purity of sulfathiazole crystals. *Org. Proc. Res. Dev.* 13:1343–56
74. Cote A, Zhou G, Stanik M. 2009. A novel crystallization methodology to ensure isolation of the most stable crystal form. *Org. Process Res. Dev.* 13:1276–83
75. Liotta V, Sabesan V. 2004. Monitoring and feedback control of supersaturation using ATR-FTIR to produce an active pharmaceutical ingredient of a desired crystal size. *Org. Process Res. Dev.* 8:488–94
76. Grön H, Borissova A, Roberts KJ. 2003. In-process ATR-FTIR spectroscopy for closed-loop supersaturation control of a batch crystallizer producing monosodium glutamate crystals of defined size. *Ind. Eng. Chem. Res.* 42:198–206
77. Gutwald T, Mersmann A. 1990. Batch cooling crystallization at constant supersaturation: technique and experimental results. *Chem. Eng. Technol.* 13:229–37
78. Nonoyama N, Hanaki K, Yabuki Y. 2006. Constant supersaturation control of antisolvent-addition batch crystallization. *Org. Process Res. Dev.* 10:727–32
79. Zhou GX, Fujiwara M, Woo XY, Rusli E, Tung H, et al. 2006. Direct design of pharmaceutical antisolvent crystallization through concentration control. *Cryst. Growth Des.* 6:892–98
80. Kee NCS, Arendt PD, Tan RBH, Braatz RD. 2009. Selective crystallization of the metastable anhydrate form in the enantiotropic pseudo-dimorph system of L-phenylalanine using concentration feedback control. *Cryst. Growth Des.* 9:3052–61
81. Kee NCS, Tan RBH, Braatz RD. 2009. Selective crystallization of the metastable α-form of L-glutamic acid using concentration feedback control. *Cryst. Growth Des.* 9:3044–51
82. Mullin JW, Nyvlt J. 1971. Programmed cooling of batch crystallizers. *Chem. Eng. Sci.* 26:369–77
83. Hermanto MW, Braatz RD, Chiu MS. 2006. A run-to-run control strategy for polymorphic transformation in pharmaceutical crystallization. *Proc. 2006 IEEE Int. Conf. Contr. Appl.*, *Munich*, *Germany*, October 4–6, pp. 1300–5. Pistcataway, NJ: IEEE Press
84. Hermanto MW, Braatz RD, Chiu MS. 2011. Integrated batch-to-batch and nonlinear model predictive control for polymorphic crystallization in pharmaceutical crystallization. *AIChE J.* 57:1008–19
85. Abu Bakar MR, Nagy ZK, Saleemi AN, Rielly CD. 2009. The impact of direct nucleation control on crystal size distribution in pharmaceutical crystallization processes. *Cryst. Growth Des.* 9:1378–84
86. Wang F, Wachter JA, Antosz FJ, Berglund KA. 2000. An investigation of solvent mediated polymorphic transformation of progesterone using in situ Raman spectroscopy. *Org. Process Res. Dev.* 4:391–95
87. Braatz RD, Fujiwara M, Wubben T, Rusli E. 2006. Crystallization: particle size control. In *Encyclopedia of Pharmaceutical Technology*, ed. J Swarbrick, pp. 858–71. New York: Marcel Dekker. 3rd ed.
88. Févotte G. 2007. In situ Raman spectroscopy for in-line control of pharmaceutical crystallization and solids elaboration processes: a review. *Chem. Eng. Res. Des.* 85:906–20
89. MacCalman ML, Roberts KJ, Kerr C, Hendriksen B. 1995. On-line processing of pharmaceutical materials using in situ X-ray diffraction. *J. Appl. Crystallogr.* 28(Pt. 5):620–22
90. Ruf A, Worlitschek J, Mazzotti M. 2000. Modeling and experimental analysis of PSD measurements through FBRM. *Part. Part. Syst. Char.* 17:167–79

86. Demonstrated in situ Raman spectroscopy for monitoring polymorphic transformation.

90. These careful experiments provided insights into the interpretation of data collected from focused beam reflectance measurement.

91. Barthe SC, Grover MA, Rousseau RW. 2008. Observation of polymorphic change through analysis of FBRM data: transformation of paracetamol from form II to form I. *Cryst. Growth Des.* 8:3316–22
92. Howard KS, Nagy ZK, Saha B, Robertson AL, Steele G. 2009. Combined PAT-solid state analytical approach for the detection and study of sodium benzoate hydrate. *Org. Proc. Res. Dev.* 13:590–97
93. Howard KS, Nagy ZK, Saha B, Robertson AL, Steele G, Martin D. 2009. A process analytical technology based investigation of the polymorphic transformations during the anti-solvent crystallization of sodium benzoate from IPA/water mixture. *Cryst. Growth Des.* 9:3964–75
94. Ono T, Kramer HJM, ter Horst JH, Jansens PJ. 2004. Process modeling of the polymorphic transformation of L-glutamic acid. *Cryst. Growth Des.* 4:1161–67
95. Hermanto MW, Kee NC, Tan RBH, Chiu MS, Braatz RD. 2008. Robust Bayesian estimation of the kinetics of the polymorphic crystallization of L-glutamic acid crystals. *AIChE J.* 54:3248–59
96. Hermanto MW, Braatz RD, Chiu MS. 2009. High-order simulation of polymorphic crystallization using weighted essentially non-oscillatory methods. *AIChE J.* 55:122–31
97. Qamar S, Noor S, Seidel-Morgenstern A. 2010. An efficient numerical method for solving a model describing crystallization of polymorphs. *Ind. Eng. Chem. Res.* 49:4940–47
98. Kee NCS, Arendt PD, Goh LM, Tan RBH, Braatz RD. 2011. Nucleation and growth kinetics estimation for L-phenylalanine hydrate and anhydrate crystallization. *CrystEngComm* 13:1197–209
99. Kee NCS, Tan RBH, Braatz RD. 2011. Semiautomated identification of the phase diagram for enantiotropic crystallizations using ATR-FTIR spectroscopy and laser backscattering. *Ind. Eng. Chem. Res.* 50:1488–95
100. Hermanto MW, Chiu MS, Braatz RD. 2009. Nonlinear model predictive control for the polymorphic crystallization of L-glutamic acid crystals. *AIChE J.* 55:2631–45
101. Talreja S, Kim DY, Mirarefi AY, Zukoski CF, Kenis PJA. 2005. Screening and optimization of protein crystallization conditions through gradual evaporation using a novel crystallization platform. *J. Appl. Crystallogr.* 38:988–95
102. Hansen CL, Skordalakes E, Berger JM, Quake SR. 2002. A robust and scalable microfluidic metering method that allows protein crystal growth by free interface diffusion. *Proc. Natl. Acad. Sci. USA* 99:16531–36
103. Kim K, Lee IS, Centrone A, Hatton AT, Myerson AS. 2009. Formation of nanosized organic molecular crystals on engineered surfaces. *J. Am. Chem. Soc.* 131:18212–13
104. Li L, Ismagilov RF. 2010. Protein crystallization using microfluidic technologies based on valves, droplets and SlipChip. *Annu. Rev. Biophys.* 39:139–58
105. Midler M, Paul EL, Whittington EF, Futran M, Liu PD, et al. 1994. Crystallization method to improve crystal structure and size. *U.S. Patent No. 5,314,506*
106. am Ende DJ, Crawford TC, Weston NP. 2003. Reactive crystallization method to improve particle size. *U.S. Patent No. 6,558,435*
107. Dauer R, Mokrauer JE, McKeel WJ. 1996. Dual jet crystallizer apparatus. *U.S. Patent No. 5,578,279*
108. Lindrud MD, Kim S, Wei C. 2001. Sonic impinging jet crystallization apparatus and process. *U.S. Patent No. 6,302,958*
109. Woo XY, Tan RBH, Chow PS, Braatz RD. 2006. Simulation of mixing effects in antisolvent crystallization using a coupled CFD-PDF-PBE approach. *Cryst. Growth Des.* 6:1291–303
110. Woo XY, Tan RBH, Braatz RD. 2009. Modeling and computational fluid dynamics–population balance equation–micromixing simulation of impinging jet crystallizers. *Cryst. Growth Des.* 9:156–64
111. Fichthorn KA, Weinberg WH. 1991. Theoretical foundations of dynamical Monte Carlo simulations. *J. Chem. Phys.* 95:1090–96
112. Goh LM, Chen KJ, Bhamidi V, He G, Kee NCS, et al. 2010. A stochastic model for nucleation kinetics determination in droplet-based microfluidic systems. *Cryst. Growth Des.* 10:2515–21
113. Kee NCS, Woo XY, Goh LM, Rusli E, He G, et al. 2008. Design of crystallization processes from laboratory research and development to the manufacturing scale: part I. *Am. Pharm. Rev.* 11(6):110–15
114. Kee NCS, Woo XY, Goh LM, Rusli E, He G, et al. 2008. Design of crystallization processes from laboratory research and development to the manufacturing scale: part II. *Am. Pharm. Rev.* 11(7):66–74
115. Knezic D, Zaccaro J, Myerson AS. 2004. Nucleation induction time in levitated droplets. *J. Phys. Chem. B* 108:10672–77

105. Demonstrated the application of dual-impinging jet crystallization to generate crystals of highly uniform size.

116. Kreutz JE, Li L, Roach LS, Hatakeyama T, Ismagilov RF. 2009. Laterally mobile, functionalized self-assembled monolayers at the fluorous-aqueous interface in a plug-based microfluidic system: characterization and testing with membrane protein crystallization. *J. Am. Chem. Soc.* 131:6042–43
117. Singh A, Lee IS, Myerson AS. 2009. Concomitant crystallization of ROY on patterned substrates: using a high throughput method to improve the chances of crystallization of different polymorphs. *Cryst. Growth Des.* 9:1182–85
118. Doki N, Seki H, Takano K, Asatani H, Yokota M, Kubota N. 2004. Process control of seeded batch cooling crystallization of the metastable α-form glycine using an in-situ ATR-FTIR spectrometer and an in-situ FBRM particle counter. *Cryst. Growth Des.* 4:949–53
119. Woo XY, Nagy ZK, Tan RBH, Braatz RD. 2009. Adaptive concentration control of cooling and anti-solvent crystallization with laser backscattering measurement. *Cryst. Growth Des.* 9:182–91
120. Kim JW, Kim JK, Kim HS, Koo KK. 2011. Application of internal seeding and temperature cycling for reduction of liquid inclusion in the crystallization of RDX. *Org. Process Res. Dev.* 15:602–9
121. Saleemi A, Nagy ZK, Rielly C. 2010. Application of direct nucleation control approach on laboratory and pilot scale crystallisation using FBRM. *Proc. Int. Workshop Ind. Cryst., 17th, Halle-Wittenberg, Germany*, Sep. 8–10, pp. 426–33. Göttingen, Ger.: Cuvillier Verlag
122. Saleemi A, Rielly C, Nagy ZK. 2012. Comparative investigation of supersaturation and automated direct nucleation control of crystal size distributions using ATR-UV/Vis spectroscopy and FBRM. *Cryst. Growth Des.* 12:1792–807
123. Lawton S, Steele G, Shering P, Zhao L, Laird I, Ni XW. 2009. Continuous crystallization of pharmaceuticals using a continuous oscillatory baffled crystallizer. *Org. Process Res. Dev.* 13:1357–63
124. Minsker KS, Zakharov VP, Berlin AA. 2001. Plug-flow tubular turbulent reactors: A new type of industrial apparatus. *Theor. Found. Chem. Eng.* 35:162–67
125. Alvarez AJ, Myerson AS. 2010. Continuous plug flow crystallization of pharmaceutical compounds. *Cryst. Growth Des.* 10:2219–28
126. Schiewe J, Zierenberg B. 2007. Process and apparatus for producing inhalable medicaments. *U.S. Patent No. 7,249,599*
127. Katta J, Rasmuson ÅC. 2008. Spherical crystallization of benzoic acid. *Int. J. Pharm.* 348:61–69
128. Kawashima Y. 1984. Spherical crystallization and pharmaceutical systems. *Pharm. Int.* 5(2):40–43
129. Woo XY, Tan RBH, Braatz RD. 2011. Precise tailoring of the crystal size distribution by controlled growth and continuous seeding from impinging jet crystallizers. *CrystEngComm* 13:2006–14
130. Jiang M, Fujiwara M, Wong MH, Zhu Z, Zhang J, et al. 2011. Achieving a target crystal size distribution by continuous seeding and controlled growth. *Proc. Int. Symp. Ind. Cryst., 18th, Zürich, Switzerland*, Sept. 13–16, pp. 69–70. Milano, Italy: Ass. Italiana di Ing. Chim. (AIDIC)
131. Lee K, Lee JH, Fujiwara M, Ma DL, Braatz RD. 2002. Run-to-run control of multidimensional crystal size distribution in a batch crystallizer. *Proc. Am. Contr. Conf., Anchorage, Alaska*, May 8–10, pp. 1013–18. Piscataway, NJ: IEEE Press
132. Patience DB, Rawlings JB. 2001. Particle-shape monitoring and control in crystallization processes. *AIChE J.* 47:2125–30
133. Sangwal K. 2008. *Additives and Crystallization Processes*. Chichester: Wiley
134. Févotte F, Févotte G. 2010. A method of characteristics for solving population balance equations (PBE) describing the adsorption of impurities during crystallization processes. *Chem. Eng. Sci.* 65:3191–98
135. Svang-Ariyaskul A, Koros WJ, Rousseau RW. 2009. Chiral separation using a novel combination of cooling crystallization and a membrane barrier: resolution of DL-glutamic acid. *Chem. Eng. Sci.* 64:1980–84
136. Elsner MP, Ziomek G, Seidel-Morgenstern A. 2009. Efficient separation of enantiomers by preferential crystallization in two coupled vessels. *AIChE J.* 55:640–49
137. Elsner MP, Ziomek G, Seidel-Morgenstern A. 2011. Simultaneous preferential crystallization in a coupled batch operation mode. Part II: experimental study and model refinement. *Chem. Eng. Sci.* 66:1269–84
138. Elsner MP, Ziomek G, Seidel-Morgenstern A. 2007. Simultaneous preferential crystallization in a coupled, batch operation mode—part I: theoretical analysis and optimization. *Chem. Eng. Sci.* 62:4760–69

139. Saleemi A, Rielly C, Nagy ZK. 2012. Monitoring of the combined cooling and antisolvent crystallisation of mixtures of aminobenzoic acid isomers using ATR-UV/vis spectroscopy and FBRM. *Chem. Eng. Sci.* In press
140. Nagy ZK, Baker M, Pedge N, Steele G. 2011. Supersaturation and direct nucleation control of an industrial pharmaceutical crystallization process using a crystallization process informatics system (CryPRINS). *Proc. Int. Workshop Ind. Cryst., 18th, Delft, The Netherlands*, Sept 7–9, pp. 101–6. Delft, The Netherlands: Delft Univ. Tech.

Annual Review of Chemical and Biomolecular Engineering

Volume 3, 2012

Contents

Indexes

Errata

An online log of corrections to *Annual Review of Chemical and Biomolecular Engineering* articles may be found at http://chembioeng.annualreviews.org/errata.shtml